

Gas barrier properties of bio-inspired Laponite–LC polymer hybrid films

Ulrich Tritschler^{1,5}, Igor Zlotnikov², Peter Fratzl², Helmut Schlaad³, Simon Grüner⁴ and Helmut Cölfen¹

¹ University of Konstanz, Physical Chemistry, Universitätsstraße 10, D 78457 Konstanz, Germany

² Max Planck Institute of Colloids and Interfaces, Department of Biomaterials, Research Campus Golm, D 14424 Potsdam, Germany

³ University of Potsdam, Institute of Chemistry, Karl Liebknecht Straße 24 25, D 14476 Potsdam, Germany

⁴ Material Physics, BASF SE, GMC/R B001, D 67056 Ludwigshafen, Germany

⁵ Present address: School of Chemistry, University of Bristol, Bristol BS8 1TS, UK.

E mail: simon.alexander.gruener@basf.com and helmut.coelfen@uni-konstanz.de

Keywords: gas permeation, liquid crystal, Laponite, liquid crystal polymer, bio inspired, organic inorganic composite material, self organization

Abstract

Bio-inspired Laponite (clay) liquid crystal (LC) polymer composite materials with high clay fractions (>80%) and a high level of orientation of the clay platelets, i.e. with structural features similar to the ones found in natural nacre, have been shown to exhibit a promising behavior in the context of reduced oxygen transmission. Key characteristics of these bio-inspired composite materials are their high inorganic content, high level of exfoliation and orientation of the clay platelets, and the use of a LC polymer forming the organic matrix in between the Laponite particles. Each single feature may be beneficial to increase the materials gas barrier property rendering this composite a promising system with advantageous barrier capacities. In this detailed study, Laponite/LC polymer composite coatings with different clay loadings were investigated regarding their oxygen transmission rate. The obtained gas barrier performance was linked to the quality, respective Laponite content and the underlying composite micro- and nanostructure of the coatings. Most efficient oxygen barrier properties were observed for composite coatings with 83% Laponite loading that exhibit a structure similar to sheet-like nacre. Further on, advantageous mechanical properties of these Laponite/LC polymer composites reported previously give rise to a multifunctional composite system.

Introduction

Biological materials, such as sea shell structures, strongly inspire current scientific research in both material science and the life sciences [1–4]. These organic–inorganic biocomposite materials consist of stiff and brittle mineral building blocks, which contain and are surrounded by soft and ductile organic components [2, 5–9]. The well-controlled coupling at the interface of organic and inorganic components and the hierarchical structure are two structural key elements leading to the materials' excellent mechanical properties combining high stiffness and toughness [1, 9–11]. In the case of natural nacre, which consists of more than 95% aragonite, the fracture resistance is 3000 times higher compared to pure aragonite [12]. The aragonite platelets are typically stacked and arrangements within the organic matrix ('columnar

nacre') were reported as well as a 'brick-and-mortar'-like structure ('sheet nacre') [4]. Besides the superior mechanical performance, some biomaterials also display additional functionality that includes, for example, outstanding optical [13–16] or magnetic properties [17].

Different methods were developed to mimic the defined hierarchical structure of biocomposites, often the structure of nacre, including layer-by-layer assembly [18–22], doctor-blading [23, 24], solution casting [25] or ice-templating and sintering [26, 27]. Recently, we developed a scalable, one-step self-organization concept based on liquid crystal (LC) formation for generating bio-inspired organic–inorganic composites [28]. This concept addresses both the coupling at the interface of organic and inorganic components and the hierarchical structure of both constituents. The LC polymers used for this concept were poly[2-(3-

butenyl)-2-oxazoline]s (PBOx) functionalized with pendent cholesteryl and carboxyl (*N*-Boc protected amino acid) side chains (double bonds of PBOx functionalized with ~20% cholesteryl and ~30% carboxyl groups). When dissolved in an appropriate organic solvent, the cholesteryl side chains allow the statistical polymer to form a chiral nematic lyotropic phase. And upon shearing a concentrated solution of the copolymer, lyotropic phases on the length scale of several hundreds of micrometers formed [28]. The carboxyl side chains were found to be able to bind to Laponite nanoplatelets, forming Laponite-LC polymer hybrid particles. These hybrid particles formed when adding a solution of the copolymer in DMF to an aqueous dispersion of Laponite platelets of pH 8–9, followed by exfoliation in DMF. At a pH of 8–9, the side chain carboxyl groups are supposed to be negatively charged and thus, can bind to the positively charged rims of the Laponite platelets. The fraction of free polymer chains was found to decrease with an increasing Laponite/LC polymer ratio (~28% and ~4% free polymer chains for an initial ratio of Laponite/LC polymer = 1:1 and 2:1 w/w, respectively). The composite materials were prepared by shearing a viscous Laponite/LC polymer dispersion in DMF to simultaneously induce LC formation of the organic and inorganic phases via a one-step self-organization process [28]. The anisotropic shape of the Laponite clay nanoplatelets allows them to form LC phases [29, 30]. The structure of the Laponite/LC polymer 1:1 and 2:1 w/w composites has been reported in detail and was found to be independent of the shearing method applied, i.e. either lateral or rotational shearing [28]. Quantitative birefringence imaging microscopy (Abrio) revealed the formation of hierarchical structures on the scale of tens to hundreds of micrometers. The structural features of the composites were visualized by x-ray microtomography revealing a homogenous structuring on the micron scale. On the micro- to nanometer scale the composite structure was studied by scanning electron microscopy (SEM), small angle x-ray scattering (SAXS), and transmission electron microscopy (TEM). The Laponite platelets were found to stack into columns within the polymeric LC phase and exhibit a layered structuring [28], resembling the structure of columnar nacre. Besides being fast, simple, and scalable, this concept has shown some universality to functional and even multifunctional composite systems [28, 31–33]. Hierarchically structured vanadium pentoxide-LC polymer composites organized on six levels were obtained exhibiting advantageous mechanical and good electrochromic properties [31, 32]. Furthermore, collective optical properties could be addressed by fabricating gold nanorod-LC polymer composite films [33].

Polymer films and composite films with enhanced gas barrier properties are currently subject of research in both academia and industry and are, for example, of highest interest for packaging applications and organic electronics encapsulations [34–37]. Gas permeation

refers to the transport of a low molecular weight substance through a testing material. For non-porous materials, the permeation depends on two parameters, the solubility of the respective gas within the material and its diffusion coefficient [34]. For high barrier applications, polymeric matrices and polymer based matrices were being developed, including for example ethylene-vinyl alcohol copolymers and LC polymers [34]. Important influence on the gas permeation of polymeric materials was assigned to the polymer crystallinity. While the permeant is considered to dissolve mainly in the amorphous phase, it is supposed to be unable to diffuse through the crystalline phase, which offers far less free volume for the transport of low molecular weight substances. Hence, gas permeation predominantly occurs through the amorphous phase and the respective solubility can be adjusted by the degree of polymer crystallinity. This is also the reason why polymeric LC phases are of interest regarding high barrier properties [34]. Incorporation of impermeable clays into polymeric matrices was found to drastically increase the gas barrier properties [35]. In the case of well exfoliated and oriented clay platelets dispersed within the polymeric matrix, the path length for the gas molecules diffusing through the material is significantly increased ('tortuosity effect'), leading to a decreased gas transmission rate, i.e. a reduced effective diffusion coefficient [35]. The gas permeability can be theoretically predicted by using, for example, Cussler's model [38].

A significant enhancement of oxygen gas permeation properties was achieved for composite films consisting of different polymers and montmorillonite (MMT), a natural clay very often used for the fabrication of films with a high gas barrier performance [35]. Amongst others, Ke *et al* [39] prepared MMT/poly(ethylene terephthalate) (PET) composites with a maximum of 3% MMT exhibiting enhanced gas permeation properties compared to pure PET. Sinha Ray *et al* [40] synthesized MMT/poly(lactide) (PLA) nanocomposites with 4, 5 and 7 wt% clay fractions which allow to reduce the oxygen transmission permeability to 88%, 85% and 81% compared to that of neat PLA. MMT/PLA composites up to 10 wt% clay content were prepared by Chang *et al* [41]. These composites led to a reduction of the oxygen gas permeability of less than half of the one obtained for pure PLA films. The PLA/MMT films consisting of 5 wt% clay reported by Thellen *et al* [42] exhibited a reduction in the oxygen permeation rate of up to 48% compared to the reference PLA films. In comparison with polyelectrolyte/MMT films, films consisting of polyelectrolytes and Laponite platelets, which have a much lower aspect ratio than MMT platelets, were found to exhibit much higher oxygen transmission rates [43]. In contrast, high loadings of large aspect ratio vermiculite potentially reduce the oxygen transmission by many orders of magnitude [37].

A high concentration of high-aspect ratio particles is likely to reduce gas permeability the strongest and biological composites show that such composites are possible. Thus, for transferring bio-inspired clay/polymer composites to the synthetic realm, a high fraction of exfoliated clay platelets within a polymeric matrix as well as a high degree of orientation of the clay platelets are required, both also allowing the film to act as an efficient gas barrier. The realization of clay/polymer composites exhibiting these features turned out to be highly challenging [36, 37]. Notable in this context are the bio-inspired clay/polymer composite film materials consisting of MMT and polyvinylalcohol, recently reported by Walther *et al* [24]. These composite films were fabricated by doctor-blading, papermaking or painting and exhibited highly promising gas barrier properties.

In this study, we applied our established bio-inspired concept for the synthesis of hierarchically structured composite materials to fabricate a series of bio-inspired Laponite/LC polymer composite coatings with different compositions and high clay loadings (Laponite/LC polymer = 1:1, 2:1, 5:1, and 10:1 w/w). These composite coatings as well as the pure LC polymer and Laponite clay reference coatings were investigated regarding their oxygen permeation properties. We expect that these will be influenced by the chemical and structural properties of the LC polymeric matrix, the Laponite content as well as the degree of platelet alignment within the polymeric phase. We show that the combination of these features makes our clay/polymer composite system unique, offering a great potential to develop coatings with improved gas barrier properties.

Results and discussion

The Laponite/LC polymer hybrid dispersions in DMF were synthesized according to an established procedure (see [Experimental section](#) for more details) [28]. The composite coatings, consisting of Laponite/LC polymer ratios of 1:1, 2:1, 5:1, and 10:1 w/w, as well as the pure LC polymer and pure clay reference coatings were prepared by doctor-blading on oriented polypropylene (oPP) carrier films of well-defined thickness. The measured oxygen transmission rates of these films are summarized in table 1. For the sake of clarity and better comparability between the different coatings, the transmission rates were normalized by the transmission rate of the uncoated oPP carrier film. Therefore, the normalized oxygen transmission rates (nOTRs) are restricted to values between unity and zero. The lower the nOTR, the better is the performance of the respective coating. In figure 1, the nOTR and the standard deviation of the coating thickness are illustrated for the pure LC polymer coating, the pure Laponite clay coating, and the composite coatings with different compositions (Laponite/LC polymer = 1:1,

2:1, 5:1, and 10:1 w/w). The standard deviation of the coating thickness (given in micrometer) serves as a measure for the homogeneity of the coating. A low absolute value of the standard deviation indicates a homogenous coating. For comparison, the uncoated oPP carrier film exhibits a sub-micrometer standard deviation.

For the one-layer coating with the pure LC polymer, the nOTR is reduced by ca. 20% (see figure 1, column 1 and table 1, entry 1). The rather low standard deviation of the thickness suggests a quite homogenous coating. The crystallinity induced by the cholesteryl mesogens in the polymer side-chains may lead to the observed enhanced gas barrier performance. For the composite coatings with the lowest clay fraction (Laponite/LC polymer 1:1 w/w), the nOTR is only reduced to below 0.8 for multiple-layered coatings (figure 1, column 2b; curing time of 30 min between the layering steps). The nOTR of the Laponite/LC polymer 1:1 w/w one-layer coating (figure 1, column 2a) is similar to the one found for the pure polymer coating (figure 1, column 1), despite of curing the composite film at 100 °C. The increased standard deviation of the coating thickness of the Laponite/LC polymer 1:1 w/w coatings compared to the pure polymer coating suggests the presence of defects such as pinholes in the composite coatings, which may have a significant influence on the oxygen transmission rate. Considering this issue, consecutive coating steps were applied to cover these defects, probably leading to the increased coating performance observed for the multiple-layered coatings. A potential negative effect of the viscosity of the Laponite/LC polymer fluid on the quality of the composite coating was addressed by fabricating a composite coating by spin-coating using a more diluted Laponite/LC polymer 1:1 w/w coating solution (table 1, entry 5). However, this coating method did not result in composite coatings with a lower nOTR and thus, an increased barrier performance compared to the doctor-blading method.

When further increasing the Laponite loading to a ratio of Laponite/LC polymer 2:1 w/w, composite coatings with a significantly decreased nOTR were obtained for the multiple-layered coatings (figure 1, column 3b). Obviously, the nOTR is highly dependent on the curing time between the coating steps since an increased barrier performance of the Laponite/LC polymer 2:1 w/w coatings compared to the Laponite/LC polymer 1:1 w/w coatings is only observed for a curing time of 90 min (figure 1, column 3a, curing time of 30 min versus column 3b, curing time of 90 min; and see table 1, entries 6 and 7).

The most efficient gas barrier was observed for composite coatings with an even higher Laponite loading of Laponite/LC polymer 5:1 w/w. For these coatings, the nOTR was decreased to ~ 0.3 corresponding to an oxygen transmission rate of $\sim 500 \text{ cm}^2 \text{ m}^{-2} \text{ d}^{-1}$, independent of the curing time (30 or 90 min; figure 1, columns 4a and b). Notably, the standard deviation of

Table 1. Details of composite coatings as well as polymer and clay reference coatings prepared on oPP films^a.

| entry | Laponite/polymer ratio of coating (w/w) | Film thickness [μm] | Standard deviation of coating thickness | OTR [$\text{cm}^2/\text{m}^2/\text{day}$] | nOTR | Coating preparation | | |
|-------|---|----------------------------------|---|---|-----------------|-----------------------------------|--|------------------------------------|
| | | | | | | Preparation method ^{b,c} | Number of layers (with blader height for the respective coating step [μm]) ^d | Curing time between layering [min] |
| 1-1 | pure LC polymer | 23.9 \pm 0.3 | 0.60 | 1242 \pm 62 | 0.79 \pm 0.06 | db | 1 (500) | - |
| 1-2 | | 24.1 \pm 0.6 | | 1366 \pm 68 | | | | |
| 2-1 | 1 : 1 | 25.8 \pm 1.5 | 2.58 | 1148 \pm 44 | 0.83 \pm 0.05 | db ^e | 1 (150) | - |
| 2-2 | | 24.6 \pm 1.6 | | 1222 \pm 46 | | | | |
| 3-1 | 1 : 1 | 26.9 \pm 4.8 | 2.58 | 845 \pm 32 | 0.52 \pm 0.03 | db | 3 (250 - 300 - 350) | 30 |
| 3-2 | | 30.2 \pm 3.3 | | 841 \pm 32 | | | | |
| 4-1 | 1 : 1 | 23.1 \pm 1.3 | 2.58 | 1534 \pm 58 | 0.94 \pm 0.07 | db | 3 (250 - 250 - 350) | 90 |
| 4-2 | | 24.5 \pm 3.1 | | n.d. | | | | |
| 5-1 | 1 : 1 | 26.8 \pm 4.2 | 2.58 | 1396 \pm 53 | 0.90 \pm 0.06 | sc | 3 | <1 |
| 5-2 | | 24.0 \pm 3.4 | | 1547 \pm 59 | | | | |
| 6-1 | 2 : 1 | 24.5 \pm 3.1 | 3.93 | 1360 \pm 52 | 0.83 \pm 0.05 | db | 3 (250 - 250 - 350) | 30 |
| 6-2 | | 24.5 \pm 2.4 | | 1361 \pm 52 | | | | |
| 7-1 | 2 : 1 | 27.7 \pm 1.9 | 3.93 | 669 \pm 25 | 0.47 \pm 0.03 | db | 3 (250 - 250 - 350) | 90 |
| 7-2 | | 31.4 \pm 8.4 | | 983 \pm 37 | | | | |
| 8-1 | 5 : 1 | 28.1 \pm 4.9 | 3.10 | 500 \pm 25 | 0.30 \pm 0.02 | db | 3 (250 - 250 - 350) | 30 |
| 8-2 | | 24.6 \pm 2.0 | | 473 \pm 23 | | | | |
| 9-1 | 5 : 1 | 29.3 \pm 3.1 | 3.10 | 608 \pm 23 | 0.35 \pm 0.02 | db | 3 (250 - 250 - 350) | 90 |
| 9-2 | | 27.2 \pm 2.3 | | 534 \pm 20 | | | | |
| 10-1 | 10 : 1 | 27.1 \pm 9.0 | 6.27 | 1375 \pm 66 | 0.88 \pm 0.06 | db | 3 (250 - 300 - 350) | 30 |
| 10-2 | | 27.4 \pm 12.1 | | 1501 \pm 73 | | | | |
| 11-1 | 10 : 1 | 25.4 \pm 1.2 | 6.27 | 1374 \pm 52 | 0.83 \pm 0.05 | db | 3 (250 - 300 - 350) | 90 |
| 11-2 | | 26.1 \pm 2.7 | | 1314 \pm 63 | | | | |
| 12-1 | pure clay | 28.0 \pm 5.0 | 12.55 | 1742 \pm 66 | 1.01 \pm 0.06 | db | 3 (250 - 300 - 350) | 30 |
| 12-2 | | 34.8 \pm 19.2 | | 1583 \pm 60 | | | | |

^aThe effective coating thickness and the normalized oxygen transmission values were obtained by referencing to the (DMF treated) oPP film (thickness: 23.3 \pm 0.8 μm , OTR: 1636 \pm 57 $\text{cm}^2 \text{m}^{-2} \text{d}^{-1}$), the error of the respective normalized transmission rate (nOTR) was obtained from the error propagation.

^bdb: doctor blading, sc: spin coating.

^cFor the coating preparation via doctor blading, the concentration was 5–8 wt% regarding the total mass for the composite and pure clay coatings and 30 wt% for the pure polymer coating.

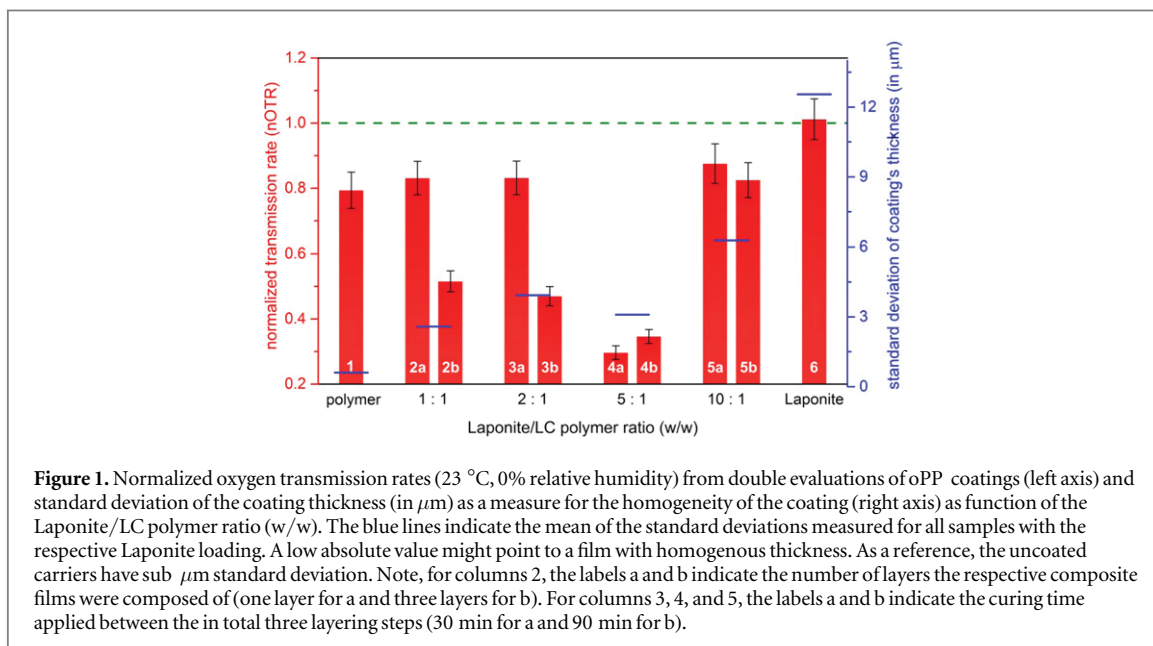
^dThe rate was adjusted to 20 mm s^{-1} for doctor blading and 1000 rpm for spin coating.

^eAdditionally cured at 100 $^{\circ}\text{C}$ for few hours after the doctor blading step.

the coating thickness reveals that the coating homogeneity is not further weakened compared to the coatings with lower Laponite loadings. Hence, at these filling degrees the positive effects, which include a reduction of free volume and an increase of tortuosity may compensate and even prevail the affected film quality. Besides the Laponite loading of the composite coatings as well as defects, such as cracks and pinholes, the gas barrier performance of the composite coatings is strongly influenced by the composite nanostructure [35, 36]. The dried Laponite/LC polymer 1:1 and 2:1 w/w composites were found to exhibit a hierarchical structure on the length scale of tens to hundreds of micrometers and feature a layered structuring. The

Laponite platelets form a columnar LC arrangement within the polymeric lyotropic phase [28]. This highly defined nano- and microstructure may support the gas barrier properties of the composite coatings, finally leading, together with an increased Laponite loading, to an increased gas barrier compared to the pure polymer coatings.

The Laponite/LC polymer 5:1 w/w composites were prepared analogously to the 1:1 and 2:1 w/w composites and, after laterally shearing the Laponite/LC polymer/DMF hybrid dispersion and drying at room temperature, the samples were structurally investigated from the millimeter to the nanometer scale by light microscopy, SEM, and SAXS analysis.



Lytotropic regions with the same structural orientation on the length scale of up to several hundreds of micrometers formed. Abrio analysis was used to quantitatively study the orientation of the composite structures on the millimeter to micrometer scale by measuring the magnitude of retardance and the azimuthal data at every pixel. Different structural orientations are illustrated by means of different colors. The color saturation corresponds to the degree of orientation, which is shown by the color wheel. For the Laponite/LC polymer 5:1 w/w composites, Abrio analysis revealed the formation of lyotropic regions with the same color, and consequently the same structural orientation, on the length scale of up to several hundreds of micrometers (see figures 2(a) and (b)) Also, as observed for the Laponite/LC polymer 1:1 and 2:1 w/w composites, the fracture surface of the Laponite/LC polymer 5:1 w/w composites exhibit a pronounced layered structure of ca. 50 nm (see SEM images, figures 2(c) and (d)).

SAXS measurements were performed with the incident x-ray beam parallel and perpendicular to the shearing direction of the Laponite/LC polymer 5:1 w/w composites at two sample–detector distances. The obtained scattering data for sample–detector distances of 28 and 107 cm was radially integrated, figures 3(a) and (b), respectively. Representative 2D SAXS data obtained at a sample–detector distance of 28 cm with the incident x-ray beam parallel and perpendicular to the shearing direction is presented in figures 3(c) and (d), respectively.

Integrated SAXS data obtained at 28 cm, when measuring parallel to the shearing direction (red line in figure 3(a)), reveal a shoulder in the Q -range of $4\text{--}5\text{ nm}^{-1}$, which is not visible when measuring perpendicular to the shearing direction (black line in figure 3(a)). This shoulder cannot be explained by the form factor of the Laponite platelets computed on the

basis of their known shape and suggests stacking of the platelets. A Kratky plot of these data, insert in figure 3(a), reveals a maximum at $Q \approx 4.5\text{ nm}^{-1}$, which corresponds to a d -spacing of $2\pi/Q \approx 1.4\text{ nm}$ ('stack of cards' model [44]). This value represents the mean spacing between the stacked clay particles and is higher compared to the d -spacing found in the analogously prepared pure Laponite reference sample [28], suggesting that the LC polymer is located between the platelets. Considering the d -spacing of the Laponite/LC polymer 2:1 and 1:1 w/w composites of 1.5 nm and 1.8 nm, respectively [28], the spacing found in the Laponite/LC polymer 5:1 w/w composites fits well to the expected distance; the lower the polymer content of the composite, the lower is the d -spacing between the Laponite platelets.

Integrated SAXS data obtained at 107 cm, when measuring perpendicular to the shearing direction (black line in figure 3(b)), reveal a shoulder at $Q \approx 0.5\text{ nm}^{-1}$, which is not visible when measuring parallel to the shearing direction (red line in figure 3(b)). This value corresponds to a d -spacing in the size range of half of the known diameter of the platelets ($\sim 12.5\text{ nm}$). For comparison, SAXS measurements of the Laponite/LC polymer 2:1 and 1:1 w/w composites revealed a shoulder at $\sim 0.25\text{ nm}^{-1}$ corresponding to a larger d -spacing of $\sim 25\text{ nm}$. This spacing is in the size range of the diameter of the Laponite platelets and was assigned to an edge-to-edge arrangement of the platelets [28]. The shoulder, currently observed in Laponite/LC polymer 5:1 w/w composites, suggests that, in average, a 'brick-and-mortar'-like nanostructure was obtained.

In addition, the 2D SAXS pattern with the incident beam perpendicular to the shearing direction is isotropic, figure 3(d), while the one obtained parallel to the shearing direction, figure 3(c), is anisotropic indicating that all the platelets lay parallel to the shearing

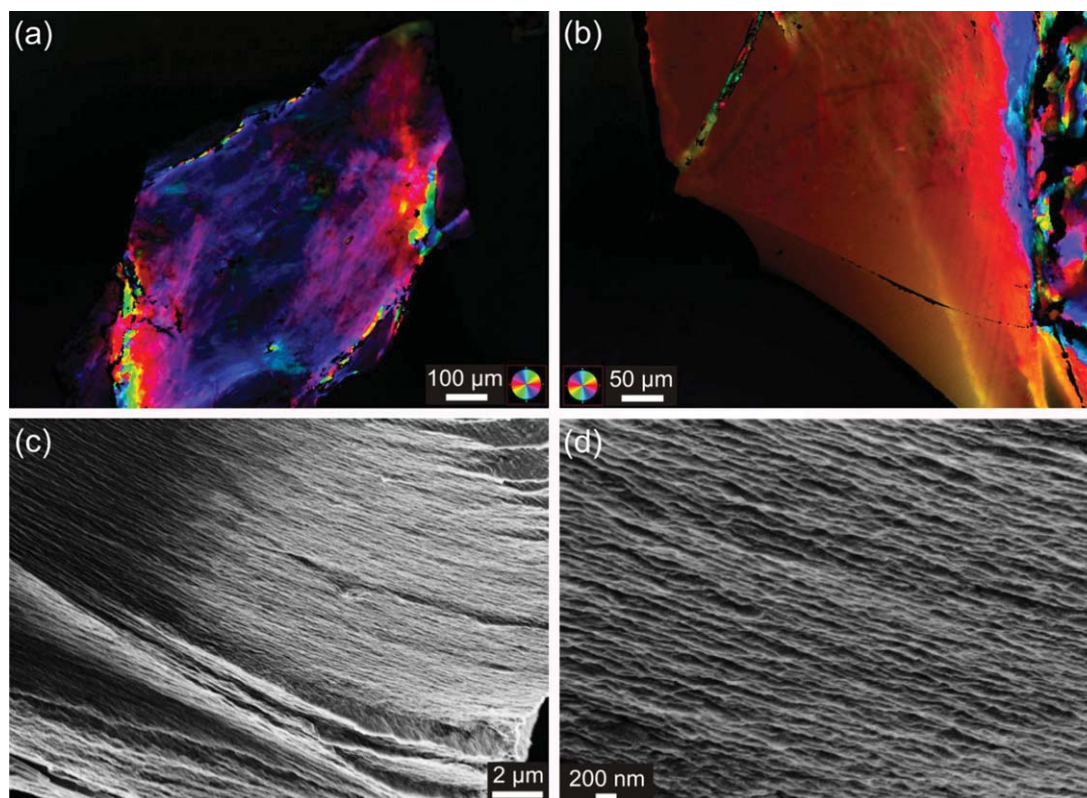


Figure 2. (a), (b) Quantitative birefringence imaging microscopy (Abrio) images of Laponite/LC polymer 5:1 w/w composites taken perpendicular to the shearing direction; (c), (d) SEM images of the fracture surface (parallel to shearing direction) of Laponite/LC polymer 5:1 w/w composites.

direction of the composite, specifically, in the horizontal plane of figure 3(c). A slight misalignment of the particles is evident from a small azimuthal intensity spread visible in figure 3(c) (dashed white line), suggesting that the platelets are also tilted with respect to the horizontal plane. This effect might be due to the low polymer content in the composites leading to insufficient particle stabilization by the LC polymer. As a result, partially positively charged rims of the Laponite platelets are free to interact with the negatively charged exposed faces of the adjacent Laponite platelets causing the observed deterioration of the nanoparticle alignment. In addition, at a Laponite content of 83%, the formation of polymeric LC phases might be hindered to some extent by the compliant inorganic phase. Although polymeric LC phases even formed when lowering the degree of cholesterol functionalization of the polymer side chains to 5% (see figure 4 in the [Experimental section](#)), the combination of both the very low polymer fraction, which may lead to the supposed partial platelet destabilization, and the high Laponite content might influence the formation of polymeric LC phases. This may potentially affect the arrangement of Laponite platelets and might induce the change of a columnar platelet arrangement within the polymeric LC phase to a 'brick-and-mortar'-like structure.

Based on the described observations, a model of a possible average nanostructure of the obtained Laponite/LC polymer 5:1 w/w composite is presented in figure 3(e). These results clearly demonstrate that the ordering and nanostructure of Laponite platelets can be influenced by varying the Laponite/LC polymer ratio. As previously shown, at lower ratios of Laponite/LC polymer 1:1 and 2:1 w/w, the Laponite platelets exhibit a columnar LC arrangement within the polymeric LC matrix [28], mimicking columnar nacre (see scheme 1, left panel). The ordering changes to a 'brick-and-mortar'-like stacking in Laponite/LC polymer 5:1 w/w composites, exhibiting a structuring observed in nature in sheet nacre (see scheme 1, right panel).

Notable in this context, the change of the arrangement of Laponite platelets within the polymeric matrix is accompanied by an increase in the path length for oxygen molecules permeating through the composite coating. This is in line with the experimental observations, revealing that probably both the composite nano-/microstructure and the Laponite loading, which increases from 50 and 67 wt% to 83 wt% (Laponite/LC polymer 1:1, 2:1, and 5:1 w/w, respectively), contribute to the enhanced gas permeation properties of the Laponite/LC polymer 5:1 w/w composite coatings compared to the Laponite/LC polymer 1:1 and 2:1 w/w composite coatings (see

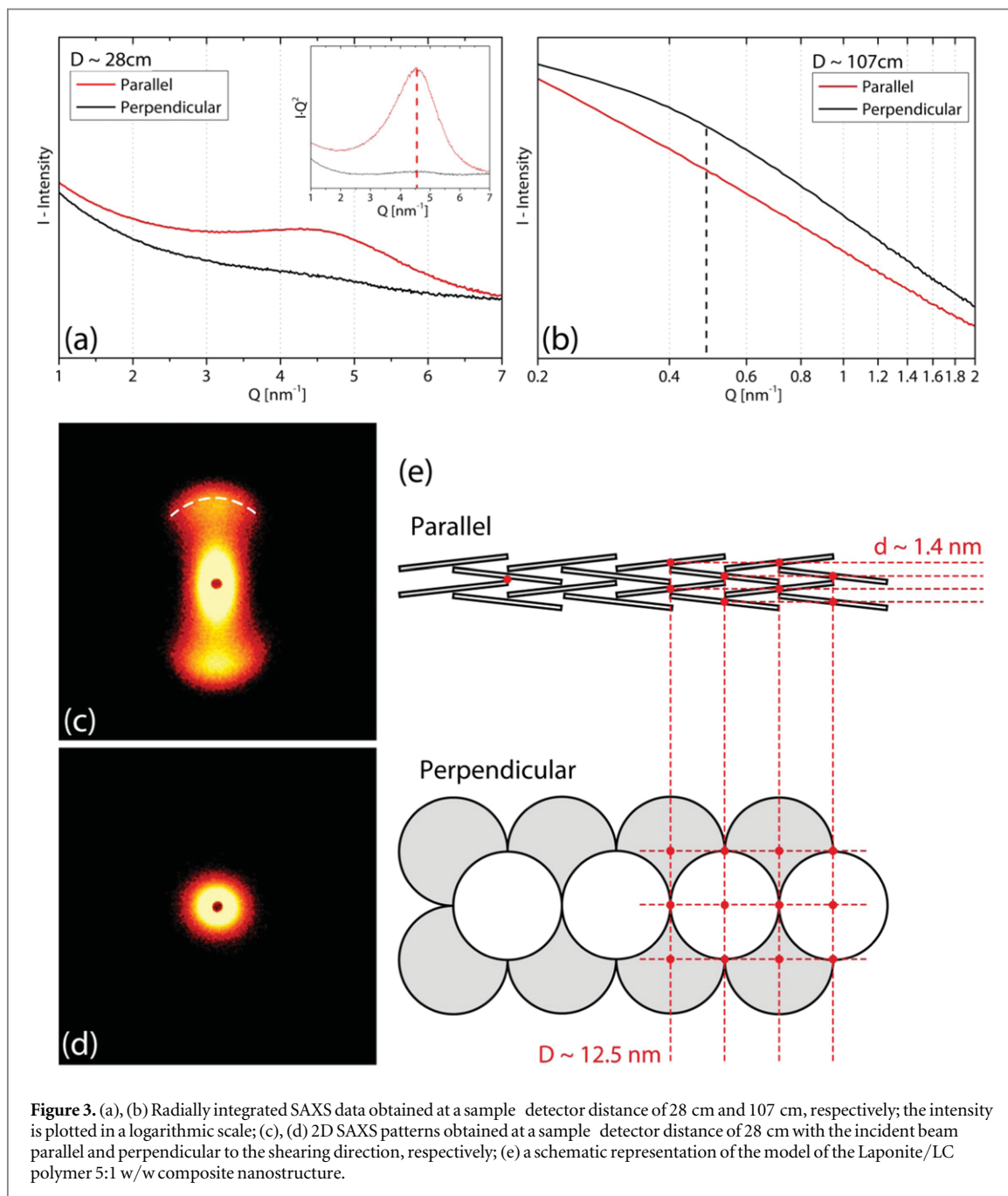
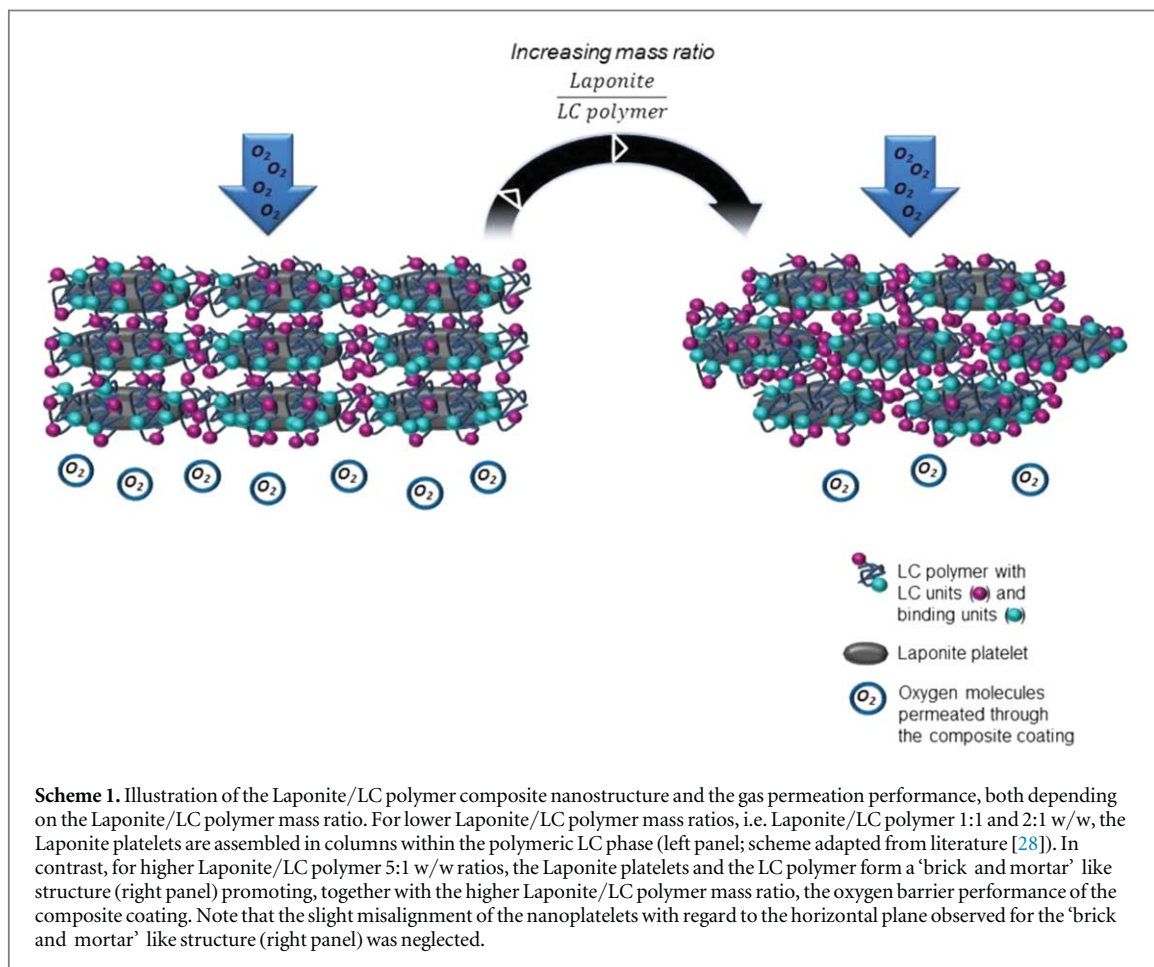


illustration of the composite nanostructure and the gas performance of the respective composite coating in scheme 1).

A further increase of the clay loading of the composite coating up to a ratio of Laponite/LC polymer 10:1 w/w leads to a substantially deteriorated film quality indicated by the doubling of the standard deviation of the coating thickness (figure 1, columns 5a and b). As a result, the nOTR increases to ca. 0.8, a level that has been already reached by the pure polymer coating. Even for the Laponite/LC polymer 10:1 w/w composites with very low polymer fractions, we still observed a pronounced hierarchical structuring on the length scale of several hundreds of micrometers, similar to the one found for the composites with higher polymer contents (data not shown). In

addition, we also observed an ordered Laponite nanostructure in the 10:1 w/w composites, however, considering the high standard deviation of the coating thickness, the coating's performance is obviously dominated by inhomogeneities and pinholes at this stage rather than by the composite nano- and micro-structure. This is in line with what can be expected for brittle composites with extremely high inorganic contents.

This conclusion is corroborated by the last set of experiments with pure clay coatings, i.e., when ultimately decreasing the polymer fraction to zero. Within the error margins the nOTR arrives at unity meaning that the permeability of the coating corresponds to the one observed for the oPP carrier film (figure 1, column 6). Together with this drastic



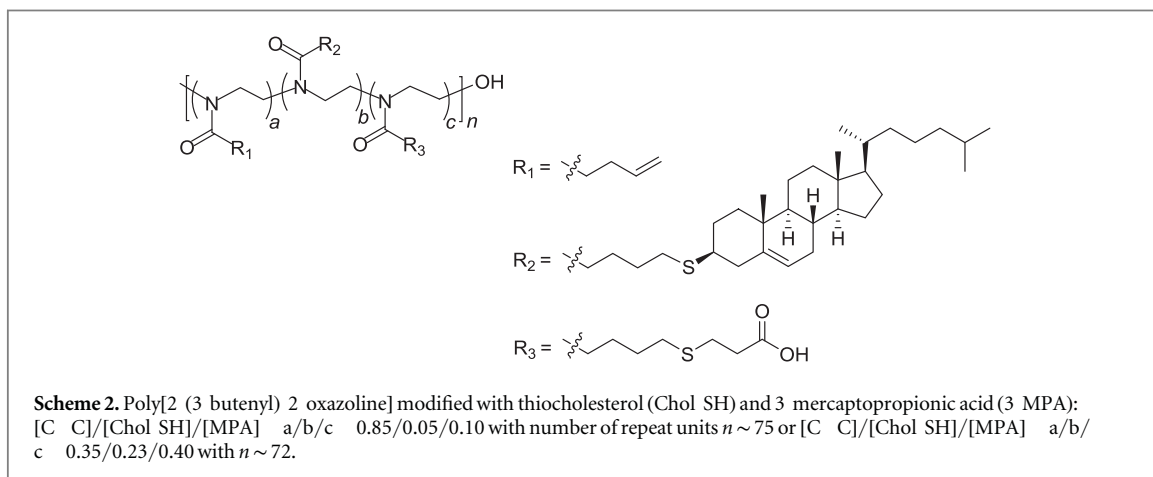
increase in gas barrier rates, a pronounced inhomogeneity of the coating is observed indicated by the high value for the standard deviation of the coating thickness. For these pure clay coatings, the Laponite platelets are supposed to be agglomerated due the positively charged rims and negatively charged surfaces, leading to the known 'house of cards' structure [45]. This might lead to coatings with considerable inhomogeneities, which significantly contribute to the experimentally observed poor standard deviation of the coating thickness. Presumably, the highly brittle, purely inorganic clay coatings lack any defined tortuous pathways for the gas molecules permeating through the coating, thus affecting directly the coating quality. Finally, permeation through the pure clay coatings probably only occurs via defects, e.g., pinholes and cracks, and the overall transmission rate is solely described by the carrier film.

The bio-inspired Laponite/LC polymer composite coatings with moderate to high Laponite loadings, in particular the composites with a maximum Laponite loading of ca. 83%, exhibit enhanced oxygen barrier properties. In a previous study [28] we investigated the mechanical performance of Laponite/LC polymer composites using nanoindentation. These results revealed that reduced elastic moduli and hardness of the composites in the direction parallel to the shearing direction (Laponite/LC polymer = 1:1 w/w (~11 and

~0.5 GPa, respectively) [28] and 2:1 w/w (~14.5 and ~0.5 GPa, respectively) [28]) and perpendicular to the shearing direction (~8.5 and ~0.45 GPa, respectively) [28] are comparable to reduced elastic moduli and hardness of human femur (measured by nanoindentation in the wet state) [46]. This shows that the bio-inspired Laponite/LC polymer composites combine both advantageous mechanical and enhanced gas permeation properties, giving rise to a multifunctional composite system.

The measured oxygen transmission rates of the Laponite/LC polymer composite coatings are higher than expected based on theoretical calculations using Cussler's model [38]⁶, suggesting that inhomogeneities and defects influence the gas permeation behavior of the composite films, even after applying multiple layering steps. Increasing the layering steps well above three might allow for more homogenous and defect-free coatings. However, for achieving significantly decreased gas permeation properties, it seems to be much more promising to use clay platelets with a considerably higher aspect ratio. Using clay platelets with higher aspect ratios than the aspect ratio of Laponite platelets may increase the tortuosity

⁶ The estimations are based on Cussler's model assuming well oriented and exfoliated clay platelets within the polymeric phase and a coating thickness of 2 μm .



effect, leading to composite films with significantly reduced gas permeation properties. This phenomenon has been already observed in the literature for different composite systems, for example, by replacing Laponite clay platelets (diameter:thickness $\sim 25:1$) [45] by MMT ($\sim 200:1$, polydisperse) [47], or vermiculite ($\sim 1100:1$) [37] clay platelets [36, 37, 43, 48–50]. By using high aspect ratio clay platelets and applying our bio-inspired LC concept onto MMT or vermiculite platelets, the resulting bio-inspired clay/LC polymer composite coatings may potentially exhibit advanced gas barrier properties, comprising advantageous features such as high inorganic clay contents of $>80\%$, stacking of the clay platelets comparable to natural nacre after particle exfoliation, and the liquid crystallinity of the polymeric matrix. While the latter LC feature of the organic phase may lead to an impermeable matrix to the oxygen molecules and thus, enhancing the coating's gas barrier performance, the first two characteristics shall allow for an increased tortuous path for the permeating low molecular weight molecules that diffuse through a staggered arrangement of impermeable clay platelets embedded in a polymeric phase [24, 34–36]. In addition to that, the film quality might be not only improved by increasing the number of composite layers but, for example, also by varying and optimizing further parameters for the film preparation, such as the deposition time, which was only recently found to be a crucial factor for the gas transmission rate [43].

Conclusion

A series of bio-inspired Laponite/LC polymer composite coatings was studied regarding their oxygen transmission properties. The LC polymer used was a polyoxazoline with pendant carboxy groups, enabling the polymer to bind to the edges of the Laponite platelets, and cholesteryl groups, which allow the polymer to form lyotropic LC phases. The polymeric LC phases represent the first factor influencing the gas

barrier properties. The Laponite/LC polymer composite coatings fabricated via a one-step self-organization process based on LC formation of the organic and the inorganic phase differ in the clay content (Laponite/LC polymer = 1:1, 2:1, 5:1 and 10:1 w/w) and the composite nanostructure (see scheme 1). The LC polymer apparently plays a dominant role in orienting the Laponite nanoplatelets. Laponite/LC polymer composite coatings with ca. 83 wt% clay content and a 'brick-and-mortar'-like structure similar to the one found in natural sheet nacre were found to exhibit the lowest oxygen transmission rates. Composite coatings with lower Laponite contents (50 and 67 wt%) far exceed the gas barrier properties of the pure LC polymer coatings. However, these composites, exhibiting a structure similar to the one found in columnar nacre, demonstrate considerably higher oxygen transmission rates than the Laponite/LC polymer 5:1 coatings. A significant drop in the gas barrier performance was observed for composite coatings with a clay content higher than ca. 83%, probably due to the presence of increasing amounts of defects and pinholes. The presented composite system might be interesting for perspective coatings, which shall combine advantageous mechanical and gas barrier properties.

Experimental section

Chemical and materials

Chemicals and solvents were purchased from several suppliers and used as received (unless otherwise noted). Aldrich: 2-chloroethylamine hydrochloride (99%), N-hydroxysuccinimide (98%), methyl triflate (99%), thiocholesterol (Chol-SH), 3-mercaptopropionic acid (3-MPA), 2,2-dimethoxy-2-phenyl acetophenone (DMPA). Alfa Aesar: 4-pentenoic acid (98%). Iris-Biotech: 1-(3-dimethylpropyl)-3-ethylcarbodiimide hydrochloride (EDAC, 99.4%). 2-(3-butenyl)-2-oxazoline was synthesized according to Gress *et al* [51]. Laponite RD was kindly donated by Rockwood Clay Additives GmbH, France.

Analytical instrumentation and methods

^1H NMR measurements were carried out at room temperature using a Bruker Avance III 400 operating at 400 MHz. CDCl_3 (purchased from Deutero GmbH, Germany) was used as solvent, and signals were referenced to $\delta = 7.26$ ppm. Gel permeation chromatography (GPC) with simultaneous UV (270 nm) and RI detection was performed in NMP (+0.5 wt % LiBr) at 70 °C, flow rate: 0.8 ml min⁻¹, using a column set of two 300 × 8 mm² PSS-GRAM columns (particle size: 7 μm, porosity: 10² and 10³ Å). Calibration was done with polystyrene standards (PSS, Mainz, Germany). MALDI-ToF MS measurements were conducted on a Bruker Microflex MALDI-TOF by using 10 μl of the polymer precursor solution (2 mg ml⁻¹ in THF), 10 μl solution of DCTB (10 mg ml⁻¹ in THF) and 1 μl of sodium trifluoroacetate (0.1 mg ml⁻¹ in acetone). Light micrographs were taken in transmission mode with a Zeiss Axio Imager.M2m microscope and a birefringence microscope (Abrio). SEM analysis was conducted on a Zeiss CrossBeam 1540XB at an acceleration voltage of 3 kV. Prior to imaging, SEM samples were sputtered with gold.

SAXS measurements were carried out using a NanoSTAR diffractometer (Bruker AXS GmbH, Karlsruhe, Germany) with a $\text{CuK}\alpha$ x-ray source and two crossed Goebel mirrors resulting in a wavelength of 0.154 nm and a beam size of approximately 400 μm in diameter. The Bruker Hi-STAR area detector was mounted at a distance of 1070 or 280 mm from the sample, which was later calibrated using crystalline silver behenate powder. The intensity was determined as a function of the scattering vector q , and corrected for background and dark current. Oxygen transmission tests were performed by means of the carrier gas method according to ASTM D-3985 at 23 °C and 0% relative humidity. The instruments for the permeation measurements used are a Mocon Oxtran 2/21 and a Mocon Oxtran 2/61. The testing area was 5 cm². The oxygen transmission rates were obtained by evaluating two different polymer coatings/composite coatings of the same composition (double evaluation). The overall thickness of the specimen was determined by means of mechanical scanning according to DIN 53370.

Polymer synthesis and modification

Polymer syntheses and modifications were performed as described elsewhere [28, 31, 51]. The polymerization of 2-(3-butenyl)-2-oxazoline (BOx) was initiated by methyl triflate (MeTf) in acetonitrile (freshly distilled from CaH_2) and stirred at 70 °C for 3 days ($[\text{BOx}]_0 = \sim 2.6$ M, $[\text{MeTf}]_0 \sim 0.03$ M). The reaction was quenched by adding 1 M aqueous NaOH, followed by stirring the mixture for another 5 h at 70 °C. The polymer was purified by dialysis against methanol (MWCO: 1 kDa) for 3 days. After evaporation of the

solvent, poly[2-(3-butenyl)-2-oxazoline] (PBOx) was freeze-dried from benzene.

PBOx used for composite coatings: number-average molar mass, $M_n = 9\,000$ g mol⁻¹ (determined by MALDI-ToF MS), dispersity, $M_w/M_n = 1.2$ (determined by GPC).

PBOx used for pure polymer coatings: $M_n = 9\,500$ g mol⁻¹ (determined by MALDI-ToF MS), $M_w/M_n = 1.3$ (determined by GPC).

Subsequently, the PBOx was modified with thiocholesterol and 3-mercaptopropionic acid by applying thiol-ene photochemistry. PBOx, Chol-SH, and 3-MPA were dissolved in dry THF. The reaction mixture was degassed, put under argon atmosphere, and exposed to UV light (Heraeus TQ 150) at room temperature for 24 h. The mixture was dialyzed against THF and ethanol (MWCO: 1 kDa), followed by evaporation of the solvent and freeze-drying of the polymer from benzene. The composition of the statistical copolymers was characterized by ^1H NMR analysis (scheme 2). ^1H NMR (400 MHz, CDCl_3) δ 0.6–2.7, 2.75 (br, SCH_2 MPA), 3.3–3.6 (br, NCH_2 backbone), 4.9–5.1 (m, $=\text{CH}_2$ BOx), 5.3 (s, $=\text{CH}-\text{Chol}$), 5.8–5.9 ($-\text{CH}=\text{BOx}$).

The composition of the modified polymer used for preparing the Laponite/LC polymer composite coatings was found to be $[\text{C}=\text{C}]/[\text{Chol}]/[\text{COOH}] = a/b/c = 0.35/0.23/0.40$ (determined by ^1H NMR). The composition of the polymer is similar to the one which was used for synthesizing and characterizing Laponite/LC polymer composites previously ($[\text{C}=\text{C}]/[\text{Chol}]/[\text{Cys}] = a/b/c = 0.51/0.21/0.28$) [28].

For the pure polymer coatings, the composition of the modified PBOx was $[\text{C}=\text{C}]/[\text{Chol}]/[\text{COOH}] = a/b/c = 0.85/0.05/0.10$ (determined by ^1H NMR). Despite the relatively low degree of cholesterol functionalization, the polymer was found to form lyotropic phases on the length scale of several hundreds of micrometers (see figure 4). Since the clay particles might influence LC formation of the polymeric matrix to some extent, thus affecting the gas permeability of the organic matrix, the LC polymers with a lower degree of cholesterol functionalization used for the pure polymer coatings compared to the LC polymers used for the composite coatings are supposed to represent a reliable reference [35, 52].

Preparation of Laponite/LC polymer composites for structural analysis

Laponite/LC polymer composites were synthesized as described previously [28]. Laponite was dispersed in MilliQ water (3 wt%, pH \sim 8–9) by ultrasonication for 30 min and subsequent stirring for 8 h. Subsequently, the respective amount of LC polymer dissolved in DMF was added while stirring (water:DMF = 2.56:1 v/v). After stirring the reaction mixture overnight to enable the nanoplatelets to bind to the polymer, water was removed by evaporation in a rotavapor at 40 °C

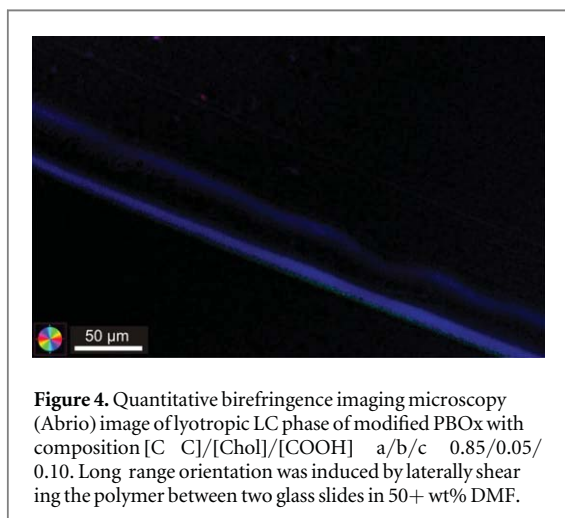


Figure 4. Quantitative birefringence imaging microscopy (Abrio) image of lyotropic LC phase of modified PBOx with composition [C C]/[Chol]/[COOH] a/b/c 0.85/0.05/0.10. Long range orientation was induced by laterally shearing the polymer between two glass slides in 50+ wt% DMF.

and 40 mbar affording a transparent viscous fluid. Laponite/LC polymer in DMF was put onto an alumina foil and sheared by either lateral shearing between two glass slides in one direction manually, lateral shearing by doctor-blading, or by rotational shearing by means of a shear cell. After shearing, the composites were dried at room temperature.

Preparation of Laponite/LC polymer composite coatings for gas permeation measurements

The Laponite–LC polymer hybrid particles for gas permeation measurements were prepared analogously to the hybrid particles for the structural analysis starting with 1–3 wt% Laponite dispersions. The composite coatings were prepared on a homogenous oPP carrier film of well-defined thickness due to difficulties to produce large-scale free-standing films (minimum surface area of 5 cm² required) with sufficient quality (i.e., with a minimum of cracks, pinholes, and inhomogeneous material thicknesses). Since the hydrophobic surface of oPP might hamper the applicability of a coating based on polar DMF, the carrier films were treated with oxygen plasma before coating. Laponite/LC polymer coatings with a surface area of at least 5 × 5 cm² were prepared on oPP by shearing the Laponite/LC polymer hybrid dispersion (ca. 5–8 wt% in DMF with respect to the total mass of Laponite and polymer) via doctor-blading. Composite coatings with one or three coating layers and different drying times between the coating steps were prepared, as specified in table 1. Reference polymer films were prepared by doctor-blading of the respective polymer dissolved in DMF (30 wt%).

Acknowledgments

The authors thank Nora Fiedler for help with polymer synthesis, Andreas Marquardt for MALDI-ToF MS measurements, and Markus Voggenreiter and Patrick

Herr for help with fabrication of some coatings. UT and HC thank BASF SE for financial support.

References

- [1] Meyers M A, McKittrick J and Chen P Y 2013 *Science* **339** 773–9
- [2] Meldrum F C and Cölfen H 2008 *Chem. Rev.* **108** 4332–432
- [3] Gao H, Ji B, Jäger I L, Arzt E and Fratzl P 2003 *Proc. Natl Acad. Sci. USA* **100** 5597–600
- [4] Wang J, Cheng Q and Tang Z 2012 *Chem. Soc. Rev.* **41** 1111–29
- [5] Lowenstam H A and Weiner S 1989 *On Biomineralization* (New York: Oxford University Press)
- [6] Fratzl P, Kolednik O, Fischer F D and Dean M N 2016 *Chem. Soc. Rev.* **45** 252–67
- [7] Dunlop J W C, Weinkamer R and Fratzl P 2011 *Mater. Today* **14** 70–8
- [8] Dunlop J W C and Fratzl P 2010 *Annu. Rev. Mater. Res.* **40** 1–24
- [9] Fratzl P and Weinkamer R 2007 *Prog. Mater. Sci.* **52** 1263–334
- [10] Aichmayer B and Fratzl P 2010 *Phys. J.* **9** 33–8
- [11] Ritchie R O 2011 *Nat. Mater.* **10** 817–22
- [12] Wegst U G K and Ashby M F 2004 *Phil. Mag.* **84** 2167–86
- [13] Gur D, Leshem B, Pierantoni M, Farstey V, Oron D, Weiner S and Addadi L 2015 *J. Am. Chem. Soc.* **137** 8408–11
- [14] Aizenberg J, Tkachenko A, Weiner S, Addadi L and Hendler G 2001 *Nature* **412** 819–22
- [15] Sundar V C, Yablont A D, Grauzl J L, Ilant M and Aizenberg J 2003 *Nature* **424** 899
- [16] Weiner S 2008 *J. Struct. Biol.* **163** 229–34
- [17] Faivre D and Schüler D 2008 *Chem. Rev.* **108** 4875–98
- [18] Tang Z, Kotov N A, Magonov S and Ozturk B 2003 *Nat. Mater.* **2** 413–8
- [19] Finnemore A, Cunha P, Shean T, Vignolini S, Guldin S, Oyen M and Steiner U 2012 *Nat. Commun.* **3** 966
- [20] Podsiadlo P, Liu Z, Paterson D, Messersmith P B and Kotov N A 2007 *Adv. Mater.* **19** 949–55
- [21] Wei H, Ma N, Shi F, Wang Z and Zhang X 2007 *Chem. Mater.* **19** 1974–8
- [22] Yeom B, Suhan K, Jinhan C, Junhee H and Kookheon C 2006 *J. Adhes.* **82** 447–68
- [23] Walther A, Bjurhager I, Malho J M, Ruokolainen J, Berglund L and Ikkala O 2010 *Angew. Chem., Int. Ed. Engl.* **49** 6448–53
- [24] Walther A, Bjurhager I, Malho J M, Pere J, Ruokolainen J, Berglund L A and Ikkala O 2010 *Nano Lett.* **10** 2742–8
- [25] Shikinaka K, Aizawa K, Fujii N, Osada Y, Tokita M, Watanabe J and Shigehara K 2010 *Langmuir* **26** 12493–5
- [26] Munch E, Launey M E, Alsem D H, Saiz E, Tomsia A P and Ritchie R O 2008 *Science* **322** 1516–20
- [27] Deville S, Saiz E, Nalla R K and Tomsia A P 2006 *Science* **311** 515–8
- [28] Tritschler U, Zlotnikov I, Zaslansky P, Aichmayer B, Fratzl P, Schlaad H and Cölfen H 2013 *Langmuir* **29** 11093–101
- [29] Nakato T and Miyamoto N 2009 *Materials* **2** 1734–61
- [30] Gabriel J C P and Davidson P 2000 *Adv. Mater.* **12** 9–20
- [31] Tritschler U, Zlotnikov I, Zaslansky P, Fratzl P, Schlaad H and Cölfen H 2014 *ACS Nano* **8** 5089–104
- [32] Tritschler U, Beck F, Schlaad H and Cölfen H 2015 *J. Mater. Chem. C.* **3** 950–4
- [33] Tritschler U, Zlotnikov I, Keckeis P, Schlaad H and Cölfen H 2014 *Langmuir* **30** 13781–90
- [34] Lagaron J M, Catalá R and Gavara R 2004 *Mater. Sci. Technol.* **20** 1–7
- [35] Pavlidou S and Papispyrides C D 2008 *Prog. Polym. Sci.* **33** 1119–98
- [36] Priolo M A, Holder K M, Guin T and Grunlan J C 2015 *Macromol. Rapid Commun.* **36** 866–79
- [37] Priolo M A, Holder K M, Greenlee S M and Grunlan J C 2012 *ACS Appl. Mater. Interfaces* **4** 529–33
- [38] Cussler E L, Hughes S E, Ward Iii W J and Aris R 1988 *J. Membr. Sci.* **38** 161–74
- [39] Ke Z and Yongping B 2005 *Mater. Lett.* **59** 3348–51

- [40] Sinha Ray S, Yamada K, Okamoto M and Ueda K 2003 *Polymer* **44** 857-66
- [41] Chang J H, An Y U and Sur G S 2003 *J. Polym. Sci. B* **41** 94-103
- [42] Thellen C, Orroth C, Froio D, Ziegler D, Lucciarini J, Farrell R, D'Souza N A and Ratto J A 2005 *Polymer* **46** 11716-27
- [43] Xiang F, Tzeng P, Sawyer J S, Regev O and Grunlan J C 2014 *ACS Appl. Mater. Interfaces* **6** 6040-8
- [44] Fratzl P, Gupta H, Paris O, Valenta A, Roschger P and Klaushofer K 2005 *Scattering Methods and the Properties of Polymer Materials* vol 130 (Berlin: Springer) pp 33-9
- [45] BYK Additives & Instruments, Laponite Performance Additives, Technical Brochure available online at (<http://byk.com/en>)
- [46] Zysset P K, Edward Guo X, Edward Hoffer C, Moore K E and Goldstein S A 1999 *J. Biomech.* **32** 1005-12
- [47] Ploehn H J and Liu C 2006 *Ind. Eng. Chem. Res.* **45** 7025-34
- [48] Guin T, Kreckler M, Hagen D A and Grunlan J C 2014 *Langmuir* **30** 7057-60
- [49] Möller M W, Kunz D A, Lunkenbein T, Sommer S, Nennemann A and Breu J 2012 *Adv. Mater.* **24** 2142-7
- [50] Kunz D A, Schmid J, Feicht P, Erath J, Fery A and Breu J 2013 *ACS Nano* **7** 4275-80
- [51] Gress A, Völkel A and Schlaad H 2007 *Macromolecules* **40** 7928-33
- [52] Osman M A, Mittal V and Lusti H R 2004 *Macromol. Rapid Commun.* **25** 1145-9